Published in final edited form as:
Bioorg Med Chem. 2009 January 15; 17(2): 548–552. doi:10.1016/j.bmc.2008.11.073.

A Novel Side-Bridged Hybrid Phosphonate/Acetate Pendant Cyclam: Synthesis, Characterization, and ^{64}Cu Small Animal PET Imaging

C. Andrew Boswell[a,†], **Celeste A. S. Regino**[b], **Kwamena E. Baidoo**[a], **Karen J. Wong**[b], **Diane E. Milenic**[a], **James A. Kelley**[c], **Christopher C. Lai**[c], and **Martin W. Brechbiel**[a,*]

a*Radioimmune & Inorganic Chemistry Section, Radiation Oncology Branch, National Cancer Institute, National Institutes of Health, Building 10 Center Drive, Bethesda, Maryland, 20892-1088*

b*Molecular Imaging Program, Center for Cancer Research, National Cancer Institute, National Institutes of Health, 10 Center Drive, Bethesda, MD 20892-1088*

c*Laboratory of Medicinal Chemistry, Center for Cancer Research, National Cancer Institute, National Institutes of Health, 376 Boyles Street, NCI-Frederick, Frederick, MD 21702*

Abstract

Copper-64 ($t_{½}$ = 12.7 hr; β^+: 0.653 MeV, 17.4%; β^-: 0.578 MeV, 39%) is produced in a biomedical cyclotron and has applications in both imaging and therapy. Macrocyclic chelators are widely used as bifunctional chelators to bind copper radionuclides to antibodies and peptides owing to their relatively high kinetic stability. A novel side-bridged cyclam featuring both pendant acetate and phosphonate groups was synthesized using a Kabachnik-Fields approach followed by hydrobromic acid deprotection. The Cu(II) complex of the novel ligand was synthesized, radiolabeling with ^{64}Cu was demonstrated, and *in vitro* (serum) stability was performed. In addition, *in vivo* distribution and clearance of the ^{64}Cu-labeled complex was visualized by positron emission tomography (PET) imaging. This novel chelate may be useful in ^{64}Cu-mediated diagnostic positron emission tomography (PET) imaging as well as targeted radiotherapeutic applications.

Keywords

positron emission tomography; copper-64; side-bridged cyclam; bifunctional chelating agent

1. INTRODUCTION

Copper-64 has favorable properties as a radionuclide for use in both positron emission tomography (PET) imaging and targeted radiotherapy due to its half-life ($t_{1/2}$ = 12.7 hr), decay characteristics (β^+ (19%); β^- (39%)) and the ability for large-scale production with high specific activity on a biomedical cyclotron.[1] Increased use of ^{64}Cu and other copper radioisotopes in nuclear medicine applications has resulted in a need for bifunctional chelators

*Correspondence to: Martin W. Brechbiel, Ph.D., Radioimmune & Inorganic Chemistry Section, Radiation Oncology Branch, NCI, NIH, Building 10, Room 1B40, 10 Center Drive, Bethesda, MD 20892-1088, Fax: (301) 402-1923, e-mail: martinwb@mail.nih.gov.
†Current address: Genentech, Inc., 1 DNA Way, MS 70, South San Francisco, CA 94080

(BFCs) that form stable radiocopper complexes and allow covalent attachment to biological molecules.[2–6] Development of optimal chelators for copper is of considerable importance when designing systems for the *in vivo* delivery of copper radioisotopes.[4,6–13]

A major class of commonly utilized chelators for labeling copper radionuclides to biomolecules comprises 1,4,8,11-tetraazacyclotetradecane-1,4,8,11-tetraacetic acid (TETA) and several structurally related analogs therein. TETA has been extensively used as a BFC for copper radionuclides in clinical imaging and therapy studies involving both antibodies and peptides.[2,14–16] Despite its widespread use, TETA is not an optimal BFC for biomedical applications. Anderson and coworkers have demonstrated the dissociation of ^{64}Cu from TETA-$_D$-Phe^1-octreotide (TETA-OC) in rat liver and subsequent binding to superoxide dismutase (SOD).[4,6,7,17,18] The current study addresses this problem through investigation of a novel side-bridged macrocyclic chelator under the hypothesis that it may provide enhanced *in vivo* stability.

Several side-bridged[19] and cross-bridged chelators[20] for Cu(II) have been described in recent years. The design of structurally pre-organized metal-chelating ligands can result in a more kinetically and/or thermodynamically stable ligand-metal complexes. Such 'structurally reinforced' macrocyclic ligands can be customized to achieve control of several parameters including flexibility/rigidity, basicity of nitrogen donors, ring size, and steric strain.[21–24] Further control over the physicochemical properties of the ligand may be achieved through the incorporation of pendant coordinating arms featuring a variety of chemical functionalities including carboxylic acid, amine, amide, sulfhydryl, and phosphonate groups.

The development of macrocyclic chelators featuring pendant phosphonate arms is an ongoing pursuit in radiopharmaceutical chemistry.[25–31] A series of methanephosphonic acid-bearing DOTA analogs - DO2P [1,4,7,10-tetraazacyclododecane-1,7-di(methanephosphonic acid)], DO3P [1,4,7,10-tetraazacyclododecane-1,4,7-tri(methanephosphonic acid)], and DOTP [1,4,7,10-tetraazacyclododecane-1,4,7,10-tetra(methanephosphonic acid)] - were all radiolabeled with ^{64}Cu in high radiochemical yields and all exhibited considerable uptake in the bone, making them potential PET bone imaging agents, as well as bone palliation and therapy agents.[29] The first synthesis of DOTP was reported in 1984.[32,33] Since then, DOTP and its monoesters have been extensively studied for their potential applications as MRI contrast agents and clinical uses as NMR shift and relaxation reagents because of the structural similarity to their DOTA analogues.

Cyclam analogs with pendant methanephosphonate arms have also been explored with a more specific focus on Cu(II) binding due to the increased selectivity of the cyclam ring system for small metal ions.[34,35] H_2TE1P (1,4,8,11-tetraazacyclotetradecan-1-yl)methyl]phosphonic acid) was found to form a very stable complex with Cu(II) (logβ(CuL) = 27.34), with a high selectivity over zinc(II) (logβ(ZnL) = 21.03) and other metal ions.[36] The crystal structure of the copper(II) complex revealed a perfect encapsulation of the central metal ion between four in plane nitrogen atoms of the macrocyclic ring and one oxygen atom of the pendant phosphonate moiety in the apical position.[36] The novel ligand presented herein, SB-TE1A1P, differs from H_2TE1P in two major respects: it contains a pendant acetate arm adjacent to the phosphonate arm, and it features an ethylene side-bridge linking two adjacent amine nitrogens.

2. RESULTS AND DISCUSSION

2.1. Ligand Synthesis

The hybrid acetate/phosphonate pendant chelator SB-TE1A1P was synthesized in 72% overall yield in two steps (Figure 1). The side-bridged cyclam, SB-TE1A,[37] was subjected to a classical Kabachnik-Fields reaction to introduce a single phosphonate ester at the secondary

amine. Both the *tert*-butyl and ethyl ester protecting groups were removed in a single step using 33% HBr in acetic acid. The monocarboxylate chelator, SB-TE1A1P, has an important potential advantage over traditional polyaminopolycarboxylate Cu(II) chelators such as TETA and DOTA in that a single carboxylic acid group can be reacted with NHS and EDC to form an active succinimidyl ester leaving the phosphonate available to bind to the radionuclide. We anticipate that SB-TE1A1P will be amenable to facile peptide or protein conjugation due to the presence of a single carboxylate group. Manning and co-workers reported the facile aqueous/organic coupling of a macrocyclic cyclen derivative bearing two phosphonate arms to a benzodiazepine receptor ligand.[38] Conjugation was achieved using a well-documented water-stable coupling agent, TSTU, which resulted in selective in situ generation of an N-hydroxysuccinimidyl ester at the single cyclen-pendant carboxylate residue in the presence of two phosphonate groups.[38]

2.2. Preparation and Characterization of Cu(II)-SB-TE1A1P

The Cu(II) complex of SB-TE1A1P was readily prepared by refluxing the neutralized acid form of the chelate with an equivalent amount of $Cu(ClO_4)_2$ in EtOH. High-resolution (FAB) mass spectrometry of the resulting blue product confirmed formation of the expected 1:1 complex. The reverse-phase HPLC of the product indicated a single peak component for this complex correlating well with the mass spectrometry result (Figure 2B). This result also correlates equally well with the reverse-phase HPLC of the ^{64}Cu-labeled complex (no-carrier-added) that gave a single radiometric peak under the same HPLC conditions (Figure 2A).

2.3. Radiochemistry and Serum Stability

Complexation of ^{64}Cu by SB-TE1A1P occurred readily to give 4.8 mCi (98% radiochemical yield) of ^{64}Cu-SB-TE1A1P at a specific activity of 39 mCi/μmol (based on the amount of ligand used). The product eluted as a single radioactive peak by RP-HPLC (Figure 2A). Incubation of ^{64}Cu-SB-TE1A1P with serum demonstrated a stable complex over the 48 hr (37 °C) time frame of the experiment (Figure 3).

2.4. Small Animal Whole Body PET Imaging and Biodistribution

The mouse PET images (Figure 4) show rapid clearance with minimal bone or liver uptake and retention. The biodistribution at 4 hr demonstrates nearly complete clearance from all major organs with a %ID/g of < 0.80 (Figure 5) suggesting no transchelation occurred to blood proteins nor was Cu release observed in contrast to Cu-TETA complexes.[7,8] Interestingly, no significant level of bone accumulation of ^{64}Cu-SB-TE1A1P was observed in the *in vivo* PET imaging study, in agreement with the biodistribution data (Figure 5). This finding suggests that more than one methanephosphonate pendant arm may be necessary for bone targeting, or alternatively that the single methanephosphonate group in SB-TE1A1P did not target the hydroxyapatite of bone because it was unavailable due to ^{64}Cu(II) complexation.

3. CONCLUSIONS

A new ethylene side-bridged cyclam analog featuring one pendant acetate arm and one pendant methylenephosphonate arm has been synthesized, and its Cu(II) complex prepared. Radiolabeling with ^{64}Cu was demonstrated, and *in vitro* studies indicated stability in human serum. PET imaging in normal mice highlighted a rapid whole-body hepatobiliary and renal clearance with minimal hepatic retention, suggesting little if any transchelation into liver and blood proteins. The single acetate arm also offers a potential site for conjugation to peptides or antibodies via formation of an active hydroxysuccinimidyl ester, as others have demonstrated selective activation and conjugation of carboxylic acid groups in the presence of phosphonate groups.[39,40] Even with the single acetate arm conjugated to a peptide, the phosphonate arm is still available to coordinate Cu(II), as are the four macrocyclic amines. In

addition, Sprague and co-workers have demonstrated favorable in vivo behavior and clearance for ^{64}Cu-CB-TE2A conjugated to a peptide, which converts one coordinating carboxylate pendant arm to an amide.[39] To better understand the in vivo stability of such peptide-conjugates, cross-bridged monoamide derivatives were synthesized as models and were shown to exhibit the same hexadentate, distorted octahedral coordination geometry that was demonstrated by analogous derivatives containing both acetate arms.[40] This work may enable development of improved agents for diagnostic positron emission tomography (PET) imaging as well as targeted radiotherapeutic applications.

4. EXPERIMENTAL SECTION

4.1. General Methods

All experiments with moisture- and/or air-sensitive compounds were carried out under argon. For column chromatography, Merck 60 Silica Gel was used (70–230 mesh). Thin-layer chromatography (TLC) was performed on silica gel 60 F-254 plates from EM Reagents. All water used was purified using a Hydro Ultrapure Water Purification system (Rockville, MD).

^{1}H NMR and ^{13}C NMR spectra were obtained using a Varian Gemini 300 MHz instrument, and the chemical shifts are reported in ppm on the δ scale relative to internal TMS or TSP. Proton chemical shifts are annotated as follows: ppm (multiplicity, integration). Mass spectra were obtained on a Waters LCT Premier Time-of-Flight Mass Spectrometer using electrospray ionization (ESI/TOF/MS) operated in positive ion mode. The electrospray capillary voltage was 3 kV, and the sample cone voltage was 60 V. The desolvation temperature was 225 °C, and the desolvation gas flow rate was nitrogen at 300 L/h. Accurate masses were obtained using the lock spray mode with Leu-Enkephalin as the external reference compound. Fast-atom bombardment (FAB) mass spectra were run on a VG 7070E-HF double-focusing mass spectrometer and were obtained in positive ion mode except where noted. A sample matrix of either glycerol (GLY) or 3-nitrobenzyl alcohol (NBA) was employed and ionization was effected by a beam of xenon atoms generated in a saddle-field ion gun at 8.0 ± 0.5 kV. Nominal mass MS were obtained at a resolution of 1200, while accurate mass analysis (high resolution FAB/MS) was carried out at a resolution of approximately 5000. For the latter, a limited-range V/E scan was employed under control of a MASPEC-II data system for Windows (MasCom GmbH, Bremen, Germany). For these analyses, 1.0 μL of 1.0 N KCl in 90% MeOH/H_2O was added to the sample before mixing with NBA matrix so that the matrix-derived ions, utilized as the internal mass references for accurate mass determinations, also included K^+ adducts. In these analyses, molecular identity could usually be confirmed by formation of a $[M+K]^+$ species. Both ^{1}H and ^{13}C NMR data, in conjunction with the observed isotopic distribution of $[M+H]^+$, were used to set constraints for the calculation of all possible elemental compositions within 20 ppm of the measured accurate mass. In all cases, a unique molecular formula could be determined by consideration of the molecular ion species and appropriate fragment ions. Positive ion MALDI mass spectra were obtained on a Shimadzu-Biotech Axima-CRF time-of-flight mass spectrometer using α-cyano-4-hydroxycinnamic acid as the sample matrix. Peptide standards of appropriate molecular weight to bracket the mass of the sample were used to provide internal mass reference peaks for accurate mass measurement.

4.2. Materials

Solvents were used as purchased. *Tert*-butyl bromoacetate, triethyl phosphite, and paraformaldehyde were purchased from the Aldrich Chemical Co. 4-Carboxymethyl-1,4,8,11-tetraazabicyclo[10.2.2]hexadecane *tert*-butyl ester (**1**) (*tert*-butyl ester of SB-TE1A) was prepared as previously reported.[37]

4.3. [8-(Diethoxy-phosphorylmethyl)-1,5,8,12-tetraaza-bicyclo[10.2.2]hexadec-5-yl]-acetic acid *tert*-butyl ester (2)

To **1** (0.45 g, 1.36 mmol) was added paraformaldehyde (0.0437 g, 1.5 mmol) and triethylphosphite (0.2417 g, 1.5 mmol). The mixture was stirred for 24 hr at 25 °C under argon, after which an additional 1.1 mol equivalents of each reagent were added. The reaction was continued for an additional 48 hr at 25 °C under argon with constant stirring. Any volatiles were removed under reduced pressure, and the remaining residue was subjected to flash chromatography (isocratic: first 70% Et_2O, 30% MeOH; then 70% Et_2O, 20% MeOH, 10% NH_4OH). Progression of the colored product band down the silica column was observable to the naked eye upon initiation of the ammonia-containing mobile phase. The relevant fractions were isolated and solvent removed under reduced pressure to give **2** as a yellow oil (0.498 g, 76.9%). ^{1}H NMR (300 MHz, $CDCl_3$, TMS) δ 1.33 (t, 6H), 1.46 (s, 9H), 1.62–1.78 (m, 4H), 2.53–2.80 (m, 9H), 2.81 (s, 4H), 2.83–2.92 (m, 4H), 2.98–3.09 (d, 2H), 3.10–3.23 (m, 3H), 3.65 (s, 2H), 4.12–4.23 (m, 4H); ^{13}C NMR (75 Hz, $CDCl_3$, TMS) δ 16.64, 16.72, 23.78, 28.33, 46.31, 46.50, 47.63, 49.61, 51.11, 51.23, 52.11, 52.44, 53.22, 53.29, 53.43, 53.53, 53.93, 61.57, 61.66, 80.89, 170.99; ^{31}P NMR (121.4 Hz, $CDCl_3$, external reference of 85% H_3PO_4 in D_2O set to 0 ppm) δ 27.69. High resolution FAB/MS: calculated for $C_{23}H_{48}N_4O_5P$: 491.3369; Found, 491.3362.

4.4. (8-Phosphonomethyl-1,5,8,12-tetraaza-bicyclo[10.2.2]hexadec-5-yl)-acetic acid (SB-TE1A1P)

To **2** (0.400 g, 0.82 mmol) was added HBr (>33% in acetic acid, 5.7 M) (20 mL). The mixture was stirred for 12 hr under argon. Excess acid was removed under reduced pressure, and the product was precipitated by adding Et_2O (100 mL). The product was isolated by suction filtration, washed with Et_2O (3 × 50 mL), and dried under vacuum to give a white powder (SB-TE1A1P) (0.6254 g, 93.7%). ^{1}H NMR (300 MHz, D_2O, TSP) δ 1.80–2.45 (br m, 6H), 2.80–4.20 (br m, 22H); ^{13}C NMR (75 Hz, D_2O, TSP) δ 19.19, 19.43, 20.75, 42.89, 43.85, 44.18, 48.98, 49.19, 50.83, 51.67, 52.10, 53.68, 53.93, 170.73, 176.49. ^{31}P NMR (121.4 Hz, D_2O, TSP, external reference of 85% H_3PO_4 in D_2O set to 0 ppm) δ 14.86 (s, 1P). Elemental analysis calculated for $C_{15}H_{31}N_4O_5P(HBr)_4(HC_2H_3O_2)_2$: C, 27.87; H, 5.30; N, 6.85; P, 3.79. Found: C, 28.10; H, 5.20; N, 6.72; P, 3.63. Low-resolution MS: Calculated for $C_{15}H_{32}N_4O_5P$: 379.21; Found, 379.40.

4.5. Cu(II)-SB-TE1A1P

To SB-TE1A1P (100 mg, 122 μmol) was added 1.1 mL of 1.0 M NaOH (1.1 mmol) and 25 mL of EtOH and stirred for a few minutes until the chelate is dissolved. A solution of $CuClO_4 \cdot 6H_2O$ (34 mg, 125 μmol) in EtOH (2 mL) was added drop wise for 30 min resulting in a deep purple suspension. The mixture was then refluxed for 6 hr and cooled overnight to obtain a bluish green mixture. A small amount of the green precipitate (<5 mg) was filtered off. Solvent was removed from the remaining blue solution and the blue product was isolated using an EtOH-Et_2O solution (60 mg, 91 % yield) High-resolution MS: Calculated for $C_{15}H_{30}N_4O_5PCu$: 440.1279; Found, 440.1249.

4.6. Radiochemistry – Synthesis of ^{64}Cu-SB-TE1A1P

A 4.92 mCi aliquot of $^{64}CuCl_2$ (in 0.1 M HCl) was added to a solution of SB-TE1A1P (0.122 μg) in NH_4OAc buffer (pH 7.5) (200 μL). The solution was incubated on a thermomixer (Eppendorf, Westbury, NY) at 95 °C for 1 hr. The reaction mixture was purified through a Chelex column (Chelex 100 resin, 100–200 mesh, Na^+ form, Bio-Rad Labs, Hercules, CA) (2 mL eluted with PBS). The radiochemical yield was 98% as per the Chelex column. The specific activity was 39 mCi/μmol based on the amount of ligand employed. Analysis was performed by reverse-phase chromatography using two Gilson Model 303 pumps, a Gilson 803C

manometric module, a Gilson 811B dynamic mixer, a Knauer ultraviolet detector, and an INUS λ-Ram radioactive detector all connected through a Gilson 506C system interface module and operated by UniPoint version 1.65 software. The compound was resolved using Beckman Coulter C18 reversed-phase Ultrasphere analytical column (5 μm, 4.6 mm × 25 cm) at 1 mL/min using the following conditions: 100% H_2O for 5 min followed by a gradient from that point to 1:9 CH_3CN:H_2O over 10 min. As a reference, the cold (natural) Cu-SB-TE1A1P complex was co-injected under identical conditions. The retention time was 6 min.

4.7. Serum Stability

A 3 mCi aliquot of ^{64}Cu-SB-TE1A1P (250 μL) was added to 2.5 mL of human serum (NHS Gemini Cat# 100–110 Lot 2537 10/25/2000) or to 2.5 mL of saline in a 100-mL PCR tube for each time point. The samples were capped and placed in a humidified 5% CO_2/95% air incubator at 37 °C. At the appropriate time, samples were analyzed by SE-HPLC using the above described HPLC system in an isocratic mode with phosphate buffered saline (1X PBS) solution as the eluent (0.5 mL/min) using a Tosohaas G3000SW, 10 μM, 7,8 mm × 30 cm column (Montgomeryville, PA). The % radioactivity in protein versus in low-molecular weight species was determined by integration.

4.8. Small Animal Whole Body PET Imaging and Biodistribution

All procedures were performed in accordance with the National Institutes of Health guidelines on the use of animals in research and were approved by the Animal Care and Use Committee of the National Cancer Institute. All *in vivo* studies were performed with 6–8 week-old female athymic (nu/nu) mice (Charles River Laboratories, Wilmington, MA). For PET imaging, mice (n = 2) were chemically restrained with 2.5% isoflurane (Abbott Laboratories, NJ) in O_2 delivered using a SurgiVet Veterinary Surgical Products vaporizer (Waukesha, WI) at a flow rate of 0.8 mL/min. The mice were kept warmed using a heating pad connected to a Polystat (ColeParmer) heating recirculator. The mice received i.v. injections of ^{64}Cu-SB-TE1A1P (~100 μCi in 1X PBS, 200 μL) and were imaged using an ATLAS (Advanced Technology Laboratory Animal Scanner) PET imager with an 11.8-cm ring diameter, an 8-cm aperture, a 6-cm effective transverse field of view, and a 2-cm axial field of view. The scanner consists of 18 “phoswich” (or depth-of-interaction) detector modules surrounding the imaging volume. The spatial resolution of the system is ~1.8 mm full width at half-maximum in the central field of view when 2-dimensional ordered-subset expectation maximization (2D OSEM) reconstruction algorithm (2 iterations, 16 subsets) is used.[41] Whole body mouse images (6 bed positions at 10 minutes per position) were acquired at 1 and 4 hr time points.

For the biodistribution studies, mice were injected i.v. with approximately 7.5 μCi of ^{64}Cu-SB-TE1A1P in 200 μL of PBS. Mice were sacrificed via CO_2 inhalation at 0.5, 1, 4, 8 and 24 hour time points (n = 5 per time point). Blood and major organs were harvested, wet-weighed, and counted in a γ-scintillation counter (1480 Wizard, PerkinElmer, Shelton, CT). The percent injected dose per gram (%/ID/g) and standard deviation (SD) were calculated.

Supplementary Material

Refer to Web version on PubMed Central for supplementary material.

ACKNOWLEDGMENT

This research was supported in part by the Intramural Research Program of the NIH, National Cancer Institute, Center for Cancer Research.

REFERENCES

1. McCarthy DW, Shefer RE, Klinkowstein RE, Bass LA, Margenau WH, Cutler CS, Anderson CJ, Welch MJ. Nucl Med Biol 1997;24:35. [PubMed: 9080473]
2. Anderson CJ, Dehdashti F, Cutler PD, Schwarz SW, Laforest R, Bass LA, Lewis JS, McCarthy DW. J Nucl Med 2001;42:213. [PubMed: 11216519]
3. Anderson CJ, Jones LA, Bass LA, Sherman ELC, McCarthy DW, Cutler PD, Lanahan MV, Cristel ME, Lewis JS, Schwarz SW. J Nucl Med 1998;39:1944. [PubMed: 9829587]
4. Anderson CJ, Lewis JS. Expert Opin Therap Pat 2000;10:1057.
5. Anderson CJ, Pajeau TS, Edwards WB, Sherman ELC, Rogers BE, Welch MJ. J Nucl Med 1995;36:2315. [PubMed: 8523125]
6. Anderson CJ, Welch MJ. Chem Rev 1999;99:2219. [PubMed: 11749480]
7. Boswell CA, McQuade P, Weisman GR, Wong EH, Anderson CJ. Nucl Med Biol 2005;32:29. [PubMed: 15691659]
8. Boswell CA, Sun X, Niu W, Weisman GR, Wong EH, Rheingold AL, Anderson CJ. J Med Chem 2004;47:1465. [PubMed: 14998334]
9. Motekaitis RJ, Roger BE, Reichert DE, Martell AE, Welch MJ. Inorganic Chemistry 1996;35:3821. [PubMed: 11666570]
10. Deshpande SV, DeNardo SJ, Meares CF, McCall MJ, Adams GP, Moi MK, DeNardo GL. J Nucl Med 1988;29:217. [PubMed: 3258025]
11. Rogers BE, Anderson CJ, Connett JM, Guo LW, Edwards WB, Sherman ELC, Zinn KR, Welch MJ. Bioconj Chem 1996;7:511.
12. Mirick GR, O'Donnell RT, DeNardo SJ, Shen S, Meares CF, DeNardo GL. Nucl Med Biol 1999;26:841. [PubMed: 10628566]
13. Anderson CJ. Cancer Biother Radiopharm 2001;16:451. [PubMed: 11789022]
14. DeNardo GL, Kukis DL, Shen S, DeNardo DA, Meares CF, DeNardo SJ. Clin Cancer Res 1999;5:533. [PubMed: 10100704]
15. DeNardo GL, DeNardo SJ, Lamborn KR, Van Hoosear KA, Kroger LA. Antib Immunoconjug Radiopharm 1991;4:859.
16. DeNardo GL, DeNardo SJ, Meares CF, Kukis DL, Diril H, McCall MJ, Adams GP, Mausner LF, Moody DC, Deshpande SV. Antib Immunoconjug Radiopharm 1991;4:777.
17. Boswell CA, Sun X, Niu W, Weisman GR, Wong EH, Rheingold AL, Anderson CJ. J Med Chem 2004;47:1465. [PubMed: 14998334]
18. Bass LA, Wang M, Welch MJ, Anderson CJ. Bioconj Chem 2000;11:527.
19. Bernier N, Allali M, Tripier R, Conan F, Patinec V, Develay S, Le Baccon M, Handel H. New J Chem 2006;30:435.
20. Wong EH, Weisman GR, Hill DC, Reed DP, Rogers ME, Condon JP, Fagan MA, Calabrese JC, Lam KC, Guzei IA, Rheingold AL. J Am Chem Soc 2000;122:10561.
21. Hancock, RD. Toward more preorganized macrocycles. In: Cooper, SR., editor. Crown Compounds. New York: VCH; 1992. p. 167-190.
22. Hancock RD, Martell AE. Chem Rev 1989;89:1875.
23. Hancock RD, Maumela H, de Sousa AS. Coord Chem Rev 1996;148:315.
24. Hancock RD, Pattrick G, Wade PW, Hosken GD. Pure Appl Chem 1993;65:473.
25. Lukes I, Kotek J, Vojitisek P, Hermann P. Coord Chem Rev 2002;216–317:287.
26. Belskii YM, Polikarpov YM, Kabachnik MI. Usp Khim 1992;61:415.
27. Geraldes CFGC, Marques MPM, de Castro B, Pereira E. Eur J Inorg Chem 2000;3:559.
28. Delgado R, Felix V, Lima LMP, Price DW. Dalton Transactions 2007:2734. [PubMed: 17592589]
29. Sun X, Wuest M, Kovacs Z, Sherry AD, Motekaitis R, Wang Z, Martell AE, Welch MJ, Anderson CJ. J Biol Inorg Chem 2003;8:217. [PubMed: 12459917]
30. Li X, Zhang S, Zhao P, Kovacs Z, Sherry AD. Inorganic Chemistry 2001;40:6572. [PubMed: 11735465]
31. Belskii FI, Polikarpov YM, Kabachnik MI. Usp Khim 1992;61:415.

32. Kabachnik MI, Medved TY, Polikarpov YM, Pasechnik MP. Izv Akad Nauk SSR Ser Khim 1984;4:844.

33. Kabachnik MI, Medved TY, Polikarpov YM, Shcherbakov BK, Bel'skii FI, Matrosov EI, Pasechnik MP. Bull Acad Sci USSR 1984;33:769.

34. Kotek J, Vojitisek P, Cisarova I, Hermann P, Jurecka P, Rohovec J, Lukes I. Collect Czech Chem Commun 2000;65:1289.

35. Kotek J, Lubal P, Hermann P, Cisarova I, Lukes I, Godula T, Svobodova I, Taborsky P, Havel J. Chem Eur J 2003;9:233.

36. Fuzerova S, Kotek J, Cisarova I, Hermann P, Binnemans K, Lukes I. Dalton Trans 2005:2908. [PubMed: 16094480]

37. Silversides JD, Allan CC, Archibald SJ. Dalton Trans 2007:971. [PubMed: 17308678]

38. Manning CH, Goebel T, Marx JN, Bornhop DJ. Org Lett 2002;4:1075. [PubMed: 11922786]

39. Sprague JE, Peng Y, Sun X, Weisman GR, Wong EH, Achilefu S, Anderson CJ. Clin. Cancer Res 2004;10:8674. [PubMed: 15623652]

40. Sprague JE, Peng Y, Fiamengo AL, Woodin KS, Southwick EA, Weisman GR, Wong EH, Golen JA, Rheingold AL, Anderson CJ. J. Med. Chem 2007;50:2527. [PubMed: 17458949]

41. Defrise M, Kinahan PE, Townsend DW, Michel C, Sibomana M, Newport DF. IEEE Trans Med Imaging 1997;16:145. [PubMed: 9101324]

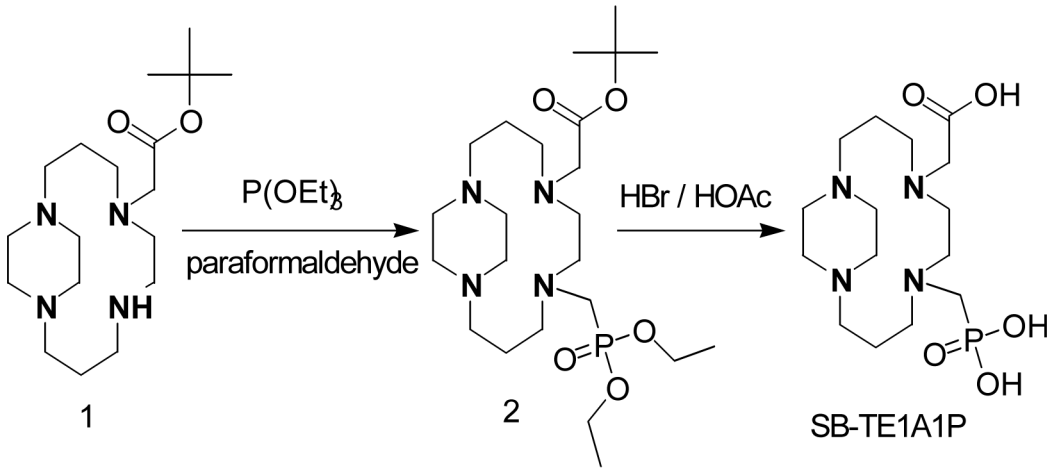

Figure 1.
Synthetic route from SB-TE1A to SB-TE1A1P.

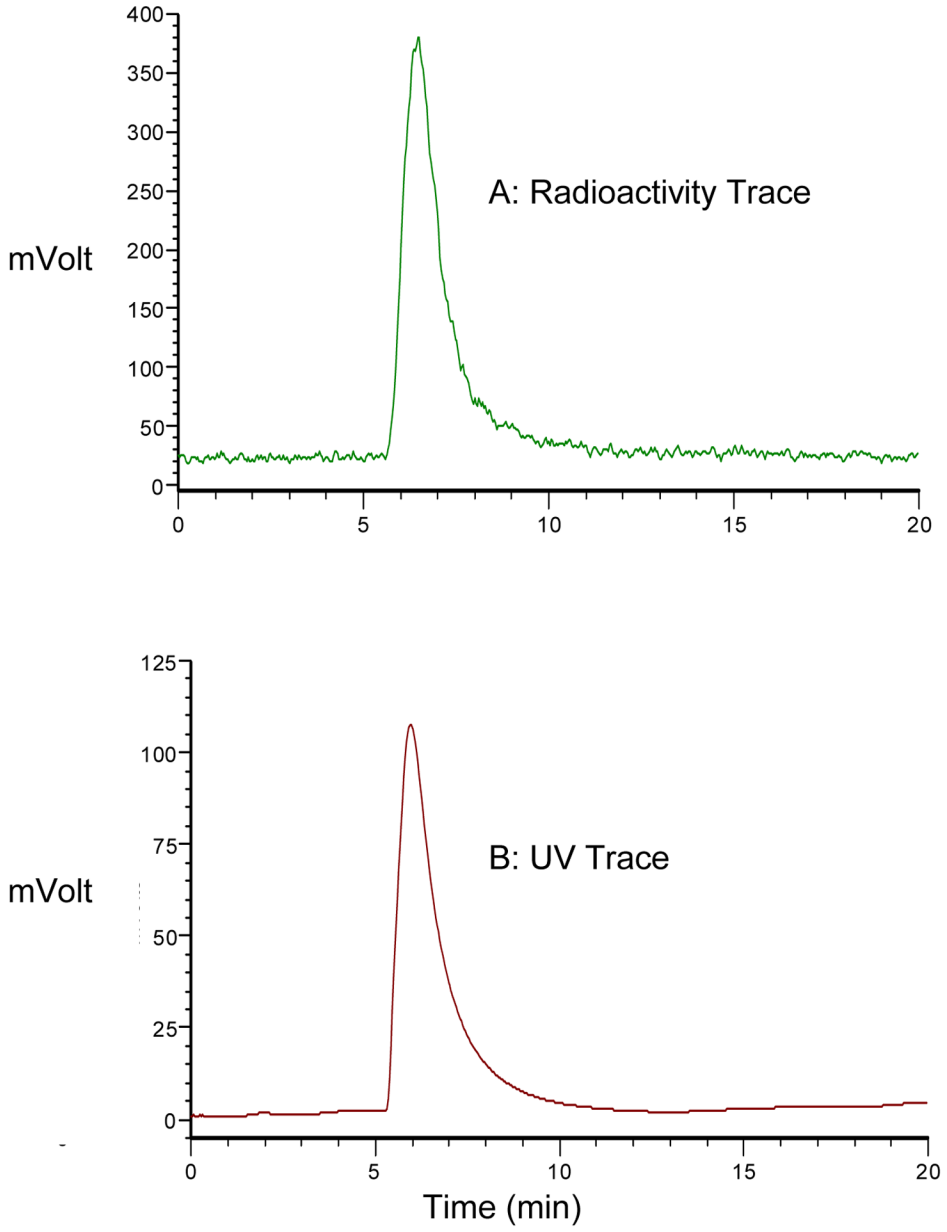

Figure 2.

HPLC chromatograms of a mixture of no-carrier added ^{64}Cu-SB-TE1A1P and ^{nat}Cu-SB-TE1A1P (A) Radiation detector and (B) UV detector RP-HPLC using a C18 reversed-phase Ultrasphere analytical column (5 μm, 4.6 mm × 25 cm) at 1 mL/min using the following conditions: 100% H_2O for 5 min followed by a gradient from that point to 1:9 CH_3CN:H_2O over 10 min.

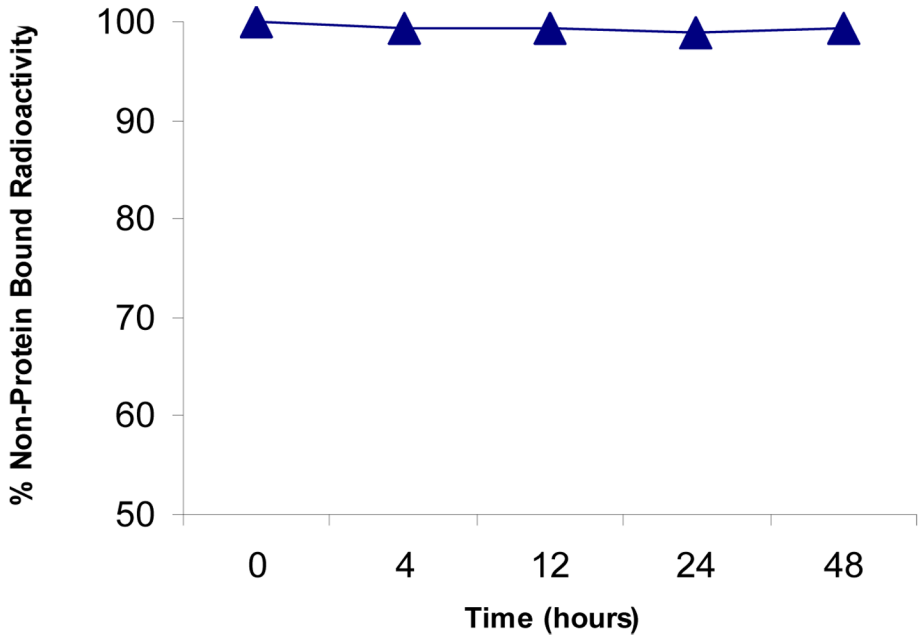

Figure 3.
Serum stability of ^{64}Cu-SB-TE1A1P at 37 °C

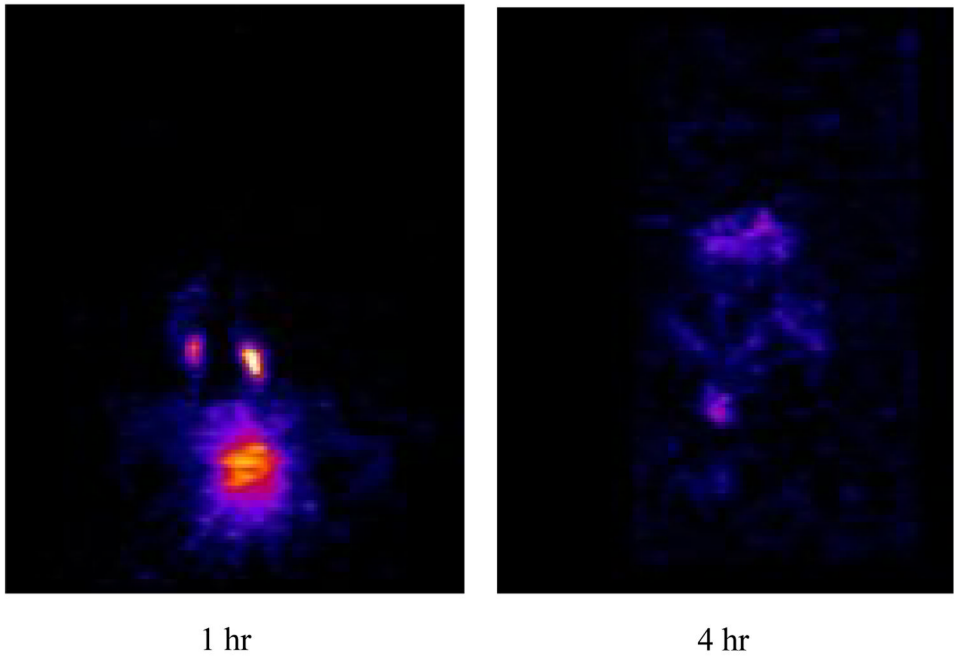

Figure 4.
Small animal PET images of normal mice at 1 and 4 hours following injection of 100 μCi ^{64}Cu-SB-TE1A1P showing majority of the agent undergoing renal and urinary clearance at 1 hr with nearly all the agent cleared 4 hr post-injection.

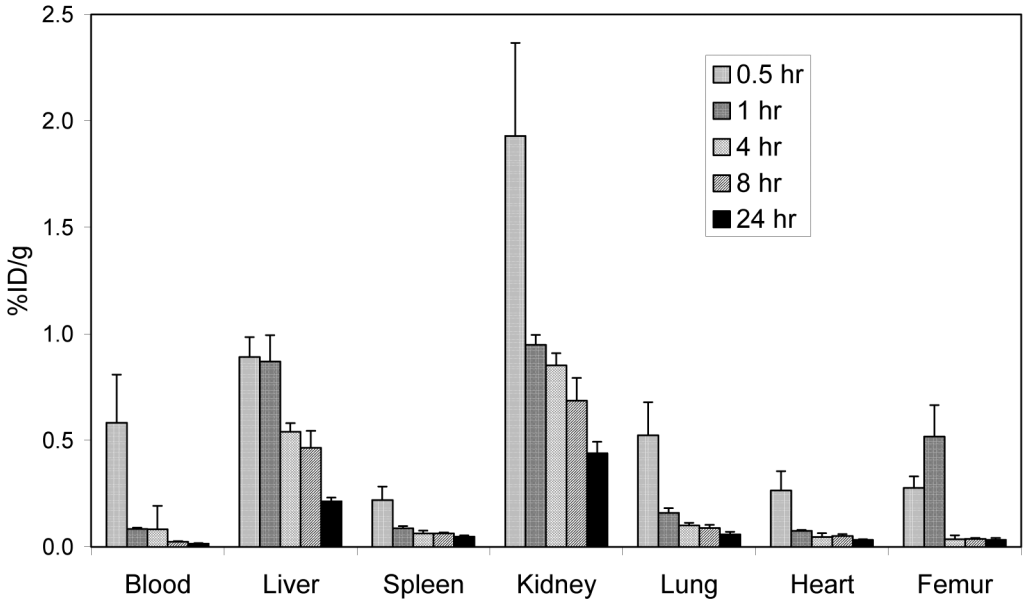

Figure 5.
Biodistribution of ^{64}Cu-SB-TE1A1P following i.v. injection in normal athymic mice